Proceedings of the TAROS (Towards Autonomous Robotic Systems) intl. conference, September 12-14, 2005, London

THE AUSTRALIAN NATIONAL UNIVERSITY

Contour Shaped Robotic Formations for Isocline Adaptation

Shahab Kalantar & Uwe R. Zimmer

Australian National University
Research School for Information Science and Engineering
and the Faculty for Engineering and Information Technology[1]
Autonomous Underwater Robotics Research Group
Canberra, ACT 0200, Australia
shahab.kalantar@rsise.anu.edu.au | uwe.zimmer@ieee.org

In this paper, we explore the possibility of applying concepts from general curve evolution theory to the decentralized control of contour-shaped formations of autonomous mobile underwater vehicles commissioned with the task of adapting to certain level sets of environmental fields created by diffusion or similar processes. The robots are assumed to be capable of measuring local gradients on their own. Controllers for individual robots are derived based on the general continuous evolution equation. Basic results on formation stability and convergence are also provided. Simulation results support the effectiveness of this approach.

1. Introduction

The spreading out of environmental chemical or biological elements, such as nutrients, smell, spores, salinity,etc., released from a source (origin), within a given space ($\Re^2$) in a medium (such as ocean or atmosphere) can often be successfully modelled by the *diffusion equation* [7]

$$\frac{\partial C(q,t)}{\partial t} = \frac{\partial}{\partial x}\left(D_x(t)\frac{\partial C(q,t)}{\partial x} + D_y(t)\frac{\partial C(q,t)}{\partial y}\right) \quad (1)$$

where $q = (x, y) \in \Re^2$, $C(q, t)$ is the concentration, D_x and D_y are diffusion rates. Solution of this equation gives the distribution at each point in time. External forces such as wind or ocean waves distort the distribution away from the ideal case. Rather than using the direct approach, simplified models are often used. One way of modelling diffusion in a natural environment is to first consider the shape of the chemical *patch* instantaneously released from a source point $q_0 = (x_0, y_0)$, and then assuming that, as the patch undergoes diffusion, distribution shape around the centre of gravity would remain unchanged (similarity hypothesis). It is common practice to assume a Gaussian distribution for the shape.

[1] *Part of this research was done under a grant from Cooperative Research Centre for Intelligent Manufacturing Systems and Technology (CRC-IMST), Australia.*

Thus, the average concentration distribution can be expressed as

$$\bar{C}(q,t) = \frac{M}{(2\pi)^{3/2}\sigma_x\sigma_y}e^{-\frac{1}{2}\left[\frac{(x-x_0)^2}{\sigma_x^2}+\frac{(y-y_0)^2}{\sigma_y^2}\right]} \quad (2)$$

where M is the mass (total number of chemical particles), and σ_x and σ_y denote standard deviations in respective directions and can, in general, be time-dependent.

In case the chemicals are released from several sources, the concentrations would add up, i.e.

$$\bar{C}(q,t) = \sum_{i=1}^{n} C_i(q - q_{0i}, t) \quad (3)$$

$\bar{C}(q, t)$ defines a *scalar field*. A *level set* (or *isocline*) of a single-source field is given by the implicit equation $\bar{C}(q, t) = C_d$, which defines the loci of points satisfying the equation

$$\frac{(x-x_0)^2}{\sigma_x^2} + \frac{(y-y_0)^2}{\sigma_y^2} = -2\ln\left(\frac{(2\pi)^{3/2}\sigma_x\sigma_y}{M}C_d\right) \quad (4)$$

(an ellipse with major axis given by

$$a_x = \sqrt{-4\sigma_x\ln\left(\frac{(2\pi)^{3/2}\sigma_x\sigma_y}{M}C_d\right)} \quad (5)$$

and similarly for the minor axis). Now, lets assume that the plume has reached its *steady state*, i.e., $C(q, t) \approx C(q, T)$ for $t \geq T$. It is often desirable to have a collection of autonomous vehicles adapt themselves to a certain level set. For instance, using such an approach, an oil leakage can be contained or a contaminated area can be decontaminated. Adaptation means that, as $t \to \infty$, we should have

$$\left|\sum_{i=0}^{N-1}\wp_i(t) + 2N\ln\frac{(2\pi)^{3/2}\sigma_x\sigma_y}{M}C_d\right| + \sum_{i=1}^{N-1}\mathcal{L}_i(t) \to \infty \quad (6)$$

where

$$\wp_i(t) = \frac{(x_i(t)-x_0)^2}{\sigma_x^2} + \frac{(y_i(t)-y_0)^2}{\sigma_y^2} \text{ and} \quad (7)$$

$$\mathcal{L}_i(t) = (\|q_i(t) - q_{i-1}(t)\| - L/N)^2 \tag{8}$$

express separation constraints between N robots R_i, $i = 0, \ldots, N-1$, whose states are denoted by $q_i(t)$.

If all the parameters of the model were known and the model described the phenomenon reasonably accurately, then the problem would be trivial. In most cases, the only information available is the local gradient of the field, $\nabla_q \bar{C}(q, t)$, acquired through on-board sensors. Thus, no a priori assumptions concerning the mathematical model of diffusion are needed (except for illustration or proving results) and the method described in this paper can cope with considerably more complex situations. Figure 1 shows a typical scenario where a group of robots have adapted to a boundary.

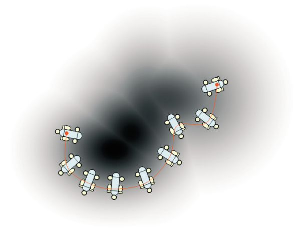

figure 1: Plume level set

When a collection of robots are to carry out a co-operative task, coordination issues are among the most important questions which have to be addressed. One of these is, naturally enough, *formation control* because the robots have to satisfy some geometric relationships in the form constraints. Most of the literature on robot formations (e.g., see [8], [9], [10]) deal with rigid ones where the robots have to maintain a rigid structure at all times. In some cases, rigidity is compromised to fulfill a particular task [15]. Recently, large formations have begun to be addressed in the literature [13]. Although not addressed extensively, deformable formations are very useful in many applications where the shape of the formation is dictated by the environment. Nevertheless, the formation, as a whole, has to balance (or, *regularize*, technically speaking) the external forces with some internal forces which strive to maintain the integrity of the formation.

A great deal of research has been done on climbing gradient fields using a formation. [14] discusses the behaviour of a swarm of robots interacting with multi-modal environments. [12] address converging to the source of an estimated plume. [4] use a small formation to localize the source of a diffusion process. The work reported in [11] is very similar to the approach we use, where it is suggested that the problem of enclosing or adapting to level sets of environmental plumes can be approached using established ideas in machine vision (edge detection). Our work is different from theirs in that we use general curve evolution rather than the classic energy-based method. Furthermore, we study formations of real robots rather than markers on an imaginary contour.

The small autonomous underwater research vehicles of the type *Serafina* (also developed at The Australian

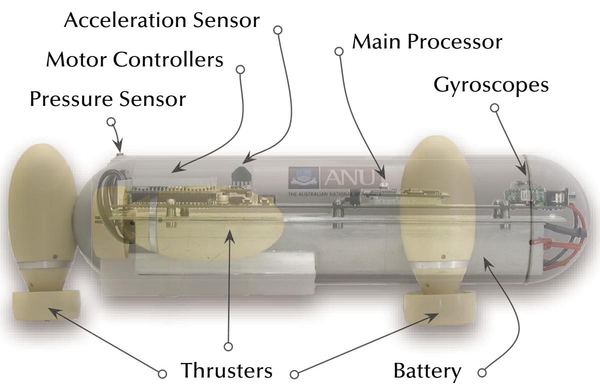

figure 2: Serafina underwater vehicle

National University) are employed as the physical realization for all considerations below. Although of compact size (overall length: 40 cm) the submersibles come with the full range of inertia sensors and short range communication channels. The basic components are depicted in figure 2, which is a photographic overlay of the outer hull and the major internal components. The propulsion system allows for a five degrees of freedom control and all axes are (almost) equally fast, while the top-speed is about 1 m/s. To learn more about the technical specfications of Serafina please refer to [16].

One control architecture for Serafinas is composed of two concurrent decoupled control modules. The depth control module keeps the robot at a certain specified distance from the bottom of the ocean by issuing appropriate torques for the three vertical thrusters. This way, the robots can be modelled as unicycles moving on a plane surface. In this paper, we are primarily concerned with the motion of robots, $\dot{q}_i(t)$, where $q_i(t)$ denotes the position in a global reference frame. We use a simple reactive controller which provides appropriate torques $\tau_L(t)$ and $\tau_R(t)$ for the two horizontal side thrusters, given a desired velocity:

$$\tau_L(t) = \Omega_L(\dot{q}_i(t)),\ \tau_R(t) = \Omega_R(\dot{q}_i(t)) \tag{9}$$

In this paper, we will not discuss the form of Ω.

2. Active contour models

Since the level sets of environmental fields are closed curves, it makes sense to apply ideas from machine vision and image processing where a deformable model (an active contour in the planar case) is adapted to a boundary by deforming an initial curve. The deformation process tries to minimize a functional which attains its minimum at the boundary. There are two different approaches to deforming a plane contour

$$\gamma(p,t) = (x_\gamma(p,t), y_\gamma(p,t))^T$$
$$\gamma\colon [0,1] \otimes \Re^+ \to \Re^2, \tag{10}$$

immersed in a field $\mathcal{F} : \Re^2 \to \Re^+$. In the classical *energy-based* method (the so-called *snake* model), the energy functional is given by

$$\begin{aligned}\mathcal{E}(\gamma(t)) &= \int_0^1 \alpha(p)\left\|\frac{\partial\gamma(p,t)}{\partial p}\right\|^2 dp \\ &+ \int_0^1 \beta(p)\left\|\frac{\partial^2\gamma(p,t)}{\partial p^2}\right\|^2 dp \\ &+ \int_0^1 \lambda(p)|\mathcal{F} - \mathcal{F}_d| dp \\ &+ \int_0^1 \mu(p)\left\|\frac{\partial^2\gamma(p,t)}{\partial t^2}\right\|^2 dp \\ &+ \int_0^1 \delta(p)\left\|\frac{\partial\gamma(p,t)}{\partial t}\right\|^2 dp\end{aligned} \tag{11}$$

where α, β, λ, μ, and δ are positive functions (usually taken to be constants) and $\mathcal{F}_d$ is a desired target concentration. The first term (*tension*) controls *tangential stretching*, the second term (*rigidity*) opposes *bending*, while the third one attracts the curve to the desired level set. In machine vision applications, $-\|\nabla_q\mathcal{F}(q)\|$ is used for the third term because boundaries are defined as points where the field changes drastically but, in this paper, the boundary of interest can be any desired concentration. The first two terms comprise the *internal energy* of the elastic band and their role is to make the curve as smooth as possible. The fourth term is the kinetic energy and the last one represents damping (energy dissipation). Using variational calculus, it is found that the curve should evolve according to the *Euler-Lagrange* partial differential equation

$$\begin{aligned}&\mu(p)\frac{\partial\gamma^2(p,t)}{\partial t^2} + \delta(p)\frac{\partial\gamma(p,t)}{\partial t} \\ &- \alpha(p)\frac{\partial\gamma^2(p,t)}{\partial p^2} + \beta(p)\frac{\partial\gamma^4(p,t)}{\partial p^4} \\ &= \mathcal{F}(\gamma(p,t)) - \mathcal{F}_d\end{aligned} \tag{12}$$

In the case of adaptation to sharp boundaries, the right hand side would be $-\|\nabla_{\gamma(p,t)}\mathcal{F}(\gamma(p,t))\|$. It is argued in [2] that setting $\beta = 0$ achieves smoothness as well, because the first *regularization* term alone penalizes curve length. Also, the kinetic and damping energy terms are not inherent to the snake model but are rather add-on's to any physical realization of active contours, so that we will drop them in the following. Moreover,

$$|\mathcal{F}(\gamma(p,t)) - \mathcal{F}_d|(-\|\nabla_{\gamma(p,t)}\mathcal{F}(\gamma(p,t))\|)$$

can be generalized by using $g(q)^2$ ($g(\|\nabla_{\gamma(p,t)}\mathcal{F}(\gamma(p,t))\|)^2$), where $g\colon [0, \max_q\mathcal{F}] \to \Re^+$ ($g\colon [0,\infty] \to \Re^+$) is a strictly decreasing function, i.e, $g(q) \to 0$ as $\mathcal{F}(q) \to \mathcal{F}_d$ ($g(\|\nabla_{\gamma(p,t)}\mathcal{F}(\gamma(p,t))\|) \to 0$ as $\|\nabla_{\gamma(p,t)}\mathcal{F}(\gamma(p,t))\| \to \infty$). Thus, the energy would simply be

$$\mathcal{E}_2(\gamma) = \alpha\int_0^1\left\|\frac{\partial\gamma(p)}{\partial p}\right\|^2 dp + \lambda\int_0^1 g(\gamma(p))^2 dp \tag{13}$$

It is further proven in [2] that minimizing $\mathcal{E}_2(\gamma)$ is the same as minimizing

$$\mathcal{E}_3(\gamma) = \int_0^1 g(\gamma(p))\left\|\frac{\partial\gamma(p)}{\partial p}\right\|^2 dp \tag{14}$$

which happens to be the problem of computing a *geodesic* in a *Riemannian* space. Now,

$$\left\|\frac{\partial\gamma(p)}{\partial p}\right\| dp = ds \tag{15}$$

is the Euclidian arc-length, so that

$$\mathcal{E}_3(\gamma) = \int_0^{L(\gamma)} g(\gamma(s))ds, \text{ where } L(\gamma) = \oint ds \tag{16}$$

is the length of γ. It can be proven [5] that the flow

$$\frac{\partial\gamma(s,t)}{\partial t} = \kappa(s,t)\vec{N}(s,t) \tag{17}$$

moves the curve in the direction of the gradient of $L(\gamma)$, i.e., reduces the length as fast as possible and is called the Euclidian *curve shortening flow*, where $\kappa(s)$ is the Euclidian curvature and $\vec{N}(s)$ is the unit inward normal to the curve at $\gamma(s,t)$. Computing the Euler-Lagrange of $\mathcal{E}_3(\gamma)$ gives the gradient descent direction of deforming an initial curve $\gamma(s,t_0)$ towards a local minimum of $\mathcal{E}_3(\gamma)$. It is proven in [2] that the evolution equation is given by

$$\begin{aligned}\frac{\partial\gamma(s,t)}{\partial t} &= g((s,t))\kappa(s,t)\vec{N}(s,t) \\ &- (\nabla_{\gamma(s,t)}g(\gamma(s,t)) \cdot \vec{N}(s,t))\vec{N}(s,t)\end{aligned} \tag{18}$$

$$\vec{N}(s,t) = \frac{(y_s(t), -x_s(t))}{\sqrt{x_s(t)^2 + y_s(t)^2}} \tag{19}$$

$$\kappa(s,t) = \frac{y_{ss}(t)x_s(t) - x_{sx}(t)y_s(t)}{(x_s(t)^2 + y_s(t)^2)^{3/2}} \tag{20}$$

where $\cdot_s = d\cdot/ds$. Usually, a constant force is also added to this equation to enable the curve to adapt to non-convex boundaries or just push it forward in the absence of gradient information. Thus,

$$\begin{aligned}\frac{\partial\gamma(s,t)}{\partial t} &= g(\gamma(s,t))(c + \kappa(s,t))\vec{N}(s,t) \\ &- (\nabla_{\gamma(s,t)}g(\gamma(s,t)) \cdot \vec{N}(s,t))\vec{N}(s,t)\end{aligned} \tag{21}$$

The evolution of the curve can also be formulated using a level-set approach (corresponding to an *Eulerian* flow in contrast with the previously discussed *Lagrangian* flow). Let γ be implicitly represented by the equation $u = 0$, where $u : \Re^2 \to \Re$. This representation is *intrinsic* (parameter-free). It is shown in [3] that u evolves according to

$$\begin{aligned}&\frac{\partial u(s,t)}{\partial t} = \\ &g(q)(c+\kappa)|\nabla_q u(q,t)| + \nabla_q g(q) \cdot \nabla_q u(q,t)\end{aligned} \tag{22}$$

where

$$\kappa = \operatorname{div}\left(\frac{\nabla_q u(q,t)}{\|\nabla_q u(q,t)\|}\right) \tag{23}$$

Equation (18) (and its equivalent equation (22)) constitute the *geodesic active contour model*. $g(\cdot)$ is called the *stopping function* because it stops the curve from evolving past the boundary. For example, in machine vision, a popular choice is

$$g(\|\nabla_q \mathcal{F}(q)\|) = 1/(1 + \|\nabla_q \mathcal{F}(q)\|^2) \tag{24}$$

It is proven in [6] that any closed plane *Jordan* curve undergoing deformation by $\partial\gamma/\partial t = k\vec{N}$ will become convex and will eventually shrink to a point, both in finite time. Similar results can be generalized to the general flow $\partial\gamma/\partial t = G(k)\vec{N}$ (G an odd function). Moreover, the length $L_\gamma(t)$ of $\gamma(t)$ evolves according to

$$\frac{dL_\gamma}{dt} = -\int_{\gamma(t)} \kappa G(\kappa) ds \tag{25}$$

In the case of an open-ended contour, the end result is a straight line, if both the end-points are kept fixed. In [2], existence, stability and uniqueness results for solutions of the geodesic active contour model are given. Finally, if $\hat{\Gamma} = \{x \in \Re^2 | g(x) = 0\}$ is a simple Jordan curve of class C^2 and $Dg(x) = 0$ on $\hat{\Gamma}$, then for a sufficiently large c,

$$\Gamma(t) = \{x \in \Re^2 | u(t, x) = 0\} \to \hat{\Gamma} \text{ as } t \to \infty \tag{26}$$

in the *Hausdorf* distance. (see [2] for proof). One last point has to be mentioned. The most general form of the evolution equation for a curve is

$$\frac{\gamma(s,t)}{\partial t} = \eta_N(s,t)\vec{N}(s,t) + \eta_T(s,t)\vec{T}(s,t) \tag{27}$$

where

$$\vec{T}(s,t) = \frac{\partial\gamma(s,t)/\partial s}{\|\partial\gamma(s,t)/\partial s\|} = \vec{N}(s,t)^\perp \tag{28}$$

is the tangent to the curve at $\gamma(s,t)$. It can be proven in [6] that the tangential component (velocity) η_T only changes the parametrization of the curve and has no effect on the geometric shape. Nevertheless, in our case (as in direct Lagrangian numerical implementation of curve evolution), a non-zero η_T is used to maintain desired separation between the robots.

3. Active contour formations

A collection of robots linked together in a chain can be made to behave like an active contour. Suppose N robots R_i, $i = 0, \ldots, N-1$, with positions denoted by $q_i(t) = [x_i, y_i)^T]$, are located on a virtual contour at time t_0. R_i can communicate with (sense) its left and right neighbors, R_{i-1} and R_{i+1}, respectively. The control rule for each robot is an approximation of equation (27) and is

$$\frac{\partial q_i(t)}{\partial t} = \eta_{N_i}(t)\vec{N}_i(t) + \eta_{T_i}(t)\vec{T}_i(t) \tag{29}$$

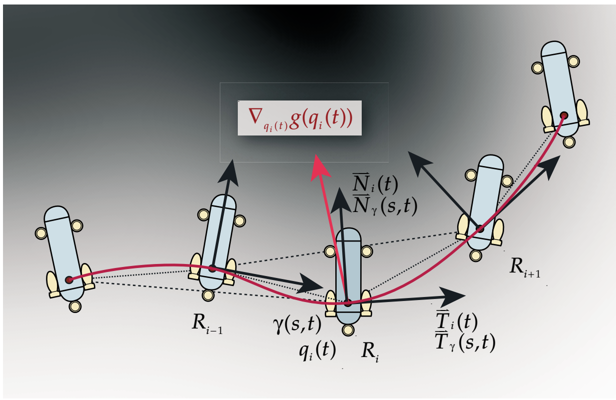

figure 3: Formation motion

where

$$\begin{aligned}\eta_{N_i}(t) &= (\alpha + \beta\kappa_i(t))g_i(t) \\ &- \langle \nabla_{q_i(t)} g(q_i(t)), \vec{N}_i(t) \rangle\end{aligned} \tag{30}$$

$$\vec{N}_i(t) = \frac{\Delta y(t) - \Delta x(t)}{\|q_{i+1}(t) - q_{i-1}(t)\|} \tag{31}$$

$$\vec{T}_i(t) = \frac{q_{i+1}(t) - q_{i-1}(t)}{\|q_{i+1}(t) - q_{i-1}(t)\|} = \vec{N}_i(t)^\perp \tag{32}$$

The curvature is approximated as

$$\kappa_i(t) = 4\frac{\Delta_{yy}(t)\Delta x(t) - \Delta_{xx}(t)\Delta y(t)}{\|q_{i+1}(t) - q_{i-1}(t)\|^3} \tag{33}$$

where

$$\begin{aligned}\Delta x(t) &= x_{i+1}(t) - x_{i-1}(t) \\ \Delta y(t) &= y_{i+1}(t) - y_{i-1}(t) \\ \Delta_{xx}(t) &= x_{i-1}(t) - 2x_i(t) + x_{i+1}(t) \\ \Delta_{yy}(t) &= y_{i-1}(t) - 2y_i(t) + y_{i+1}(t)\end{aligned} \tag{34}$$

To derive these formulas, we have used the following approximations in equations (19) and (20):

$$\begin{aligned}q_s(t) &= \frac{dq_i(t)}{ds} \approx \frac{1}{2L/N}(q_{i+1}(t) - q_{i-1}(t)) \\ q_{ss}(t) &= \frac{d^2 q_i(t)}{ds^2} \\ &\approx \frac{1}{2L/N}(q_{i+1}(t) - 2q_i(t) + q_{i-1}(t))\end{aligned} \tag{35}$$

where L is the length of the approximated contour given by

$$\sum_{i=1}^{N-1} \|q_{i+1}(t) - q_{i-1}(t)\|. \tag{36}$$

In the case of a closed contour, the boundary conditions are $q_N \equiv q_0$ and $q_{-1} \equiv q_{N-1}$. For an open contour, the control rules for the two end-point robots are

$$\begin{aligned}\dot{q}_0(t) &= -g(q_o(t))\nabla_{q_0(t)}\mathcal{F}(q_0(t)) \\ \dot{q}_{N-1}(t) &= -g(q_{N-1}(t))\nabla_{q_{N-1}(t)}\mathcal{F}(q_{N-1}(t))\end{aligned} \tag{37}$$

Thus the two end robots move freely on the gradient field. Two good candidates for $g(\cdot)$ are

$$g_1(q) = 1 - \frac{1}{1+\sigma|\mathcal{F}(q)-\mathcal{F}_d|^2}$$
$$g_2(q) = 1 - \frac{1}{\sigma\sqrt{2\pi}} e^{|\mathcal{F}(q)-\mathcal{F}_d|^2/\sigma^2} \quad (38)$$

for a desired level set $\mathcal{F}_d$. We have

$$\nabla_q g(q) = \frac{\partial g}{\partial \mathcal{F}}(q)\nabla_q \mathcal{F}(q) \quad (39)$$

and

$$\nabla_{\mathcal{F}} g_1(q) = 2(\mathcal{F}(q)-\mathcal{F}_d)(1-g_1(g))^2$$
$$\nabla_{\mathcal{F}} g_2(q) = -\frac{(\mathcal{F}(q)-\mathcal{F}_d)}{\sigma^2} g_2(g) \quad (40)$$

As can be seen in the formulas for $\vec{N}_i(t)$ and $\kappa_i(t)$, L/N has dropped out altogether. To maintain an equal distance L/N between the robots, we proposed a non-zero tangential velocity in [1]:

$$\eta_{T_i}(t) = -\zeta e^{4\frac{(q_i(t)-q_{i-1}(t))^2}{\rho_i(t)^2}} + \zeta e^{4\frac{(q_{i+1}(t)-q_i(t))^2}{\rho_i(t)^2}} \quad (41)$$

where $\rho_i(t) = \|q_{i+1}(t)-q_i(t)\| + \|q_i(t)-(q_{i-1}(t))\|$.

This, of course, does not constrain the total length of the contour, so that robots can get arbitrarily close to each other. In some applications, it might be desirable to constrain the length to some bounded interval $L_{\text{MIN}} \le L \le L_{\text{MAX}}$, which is equivalent to requiring that robots should not get closer together than $d_{\text{MIN}} = L_{\text{MIN}}/N$ and similarly for $d_{\text{MAX}} = L_{\text{MAX}}/N$. In the case of closed contours, this can be achieved by weighting the original normal velocity, i.e., replacing $\eta_{N_i}(t)$ with

$$\tilde{\eta}_{N_i}(t) = \frac{\tanh(\alpha_2\varsigma_-)\tanh(\alpha_2\varsigma_+)}{(\alpha_1\|\eta_{T_i}(t)\|^2+1)}\eta_{N_i}(t)$$
$$\varsigma_- = \|q_i(t)-q_{i-1}(t)\| - d_{\text{MIN}},$$
$$\varsigma_+ = \|q_i(t)-q_{i-1}(t)\| - d_{\text{MAX}} \quad (42)$$

In the case of open contours, a fixed distance d between robots can be maintained using the formula

$$\eta_{T_i}(t) = -\zeta e^{\frac{\|q_i(t)-q_{i-1}(t)\|^2}{\rho_i(t)^2}} + \zeta e^{\frac{\|q_{i+1}(t)-q_i(t)\|^2}{\rho_i(t)^2}} \quad (43)$$

and using the following control laws for the end robots:

$$\dot{q}_0(t) = -g(q_0(t))\nabla_{q_o(t)}\mathcal{F}(q_o(t)) \quad (44)$$
$$+ e^{\frac{(\|q_1(t)-q_0(t)\|-d)^2}{d^2}} \frac{\nabla^{\perp}_{q_0(t)}\mathcal{F}(q_0(t))}{\left\|\nabla^{\perp}_{q_0(t)}\mathcal{F}(q_0(t))\right\|}$$

$$\dot{q}_{N-1}(t) = -g(q_{N-1}(t))\nabla_{q_{N-1}(t)}\mathcal{F}(q_{N-1}(t)) \quad (45)$$
$$+ e^{\frac{(\|q_{N-1}(t)-q_{N-2}(t)\|-d)^2}{d^2}} \frac{\nabla^{\perp}_{q_{N-1}(t)}\mathcal{F}(q_{N-1}(t))}{\left\|\nabla^{\perp}_{q_{N-1}(t)}\mathcal{F}(q_{N-1}(t))\right\|}$$

It should be noted that in real applications, global coordinates are usually hard to determine, if at all possible. This, specifically, applies to underwater applications. Suppose all the calculations are done with respect to the local body-fixed coordinates Υ_i on R_i. Suppose that R_i can determine the relative position of its neighbors, denoted by $\tilde{q}_{i-1}(t)$ and $\tilde{q}_{i+1}(t)$. Then, the motion of R_i with respect to Υ_i can be expressed as

$$[\dot{x}_{\Upsilon_i(t)}, \dot{y}_{\Upsilon_i(t)}]^T = \tilde{\eta}_{\tilde{N}_i}(t)\vec{\tilde{N}}_i - \tilde{\eta}_{\tilde{T}_i}(t)\vec{\tilde{T}}_i \quad (46)$$

where the symbols with tildes are the same as given previously but with replacements $q_{i-1} \leftarrow \tilde{q}_{i-1}$, $q_{i+1} \leftarrow \tilde{q}_{i+1}$ and $q_i \leftarrow 0$ in the formulas for N_i, T_i and κ_i. Since orientation does not matter, these are the only modifications necessary to make the calculations local.

4. Formation stability and convergence

In this section, we address some theoretical issues concerning the stability of the contour formation. One way of approaching this is to choose, as a measure of stability, the distance between the formation and the ideal imaginary continuous curve. We base the analysis on ideas from [4], where a set of *virtual robots* guide a certain formation towards a local minimum of a certain field. In our case, an appropriate choice for the *web* of *virtual leaders* is the idealised curve $\gamma: [0,1] \to \Re^2$, parametrized by s. Imagine that the robots in the formation are initially distributed along this curve with equal distance from each other measured on the curve (with respect to the metric defined by ds). Let L_γ denote the length of γ which should remain fixed during evolution. Thus, the virtual leader for R_i would be $\gamma_{s_i} = \gamma(s_i)$ where

$$\int_{s_i}^{s_{i+1}} \gamma(s)ds = L_\gamma/N \quad (47)$$

Since the formation is an approximation of the ideal continuous curve, and supposing that N is large enough, the distance between two robots can be approximated by $L_\gamma/N \approx \|q_{i+1}-q_i\|$. γ evolves according to the rule

$$\gamma(s,t) = \frac{\partial\gamma(s,t)}{\partial t} = \frac{\partial\gamma(s,\tau)}{\partial\tau}\dot{\tau} \quad (48)$$

where τ parametrizes the path, $\dot{\tau} = d\tau/dt$ denotes the speed of traversal and $\partial\gamma(s,\tau)/\partial\tau$ gives the path traversed by $\gamma(s)$ and is given by

$$\begin{aligned}\dot{\gamma}_s(\tau) &= ((\alpha + \beta\kappa_s(\tau))g(\gamma_s(\tau))) \\ &- \left\langle \frac{\nabla_{\gamma_s(\tau)} g(\gamma_s(\tau))}{\|\nabla_{\gamma_s(\tau)} g(\gamma_s(\tau))\|}, N_s(\tau) \right\rangle \\ &+ \Lambda\left(s - \frac{1}{2}\right)\frac{\partial L(\tau)}{\partial\tau} T_s(\tau)\end{aligned} \tag{49}$$

for $0 < s < 1$, and

$$\begin{aligned}\dot{\gamma}_s(\tau) &= g(\gamma_s(\tau))\nabla_{\gamma_s(\tau)}\mathcal{F}(\gamma_s(\tau)) \\ &+ \Lambda\left(s - \frac{1}{2}\right)\frac{\partial L(\tau)}{\partial\tau}\nabla^{\perp}_{\gamma_s(\tau)}\mathcal{F}(\gamma_s(\tau))\end{aligned} \tag{50}$$

for $s = 0, 1$, where $\Lambda(r)$ is zero for $r = 0$, is 1 for $r > 0$, and is -1 for $r < 0$. The tangential components stretch the curve to maintain a fixed length for the curve. The robots have to remain on the curve, while maintaining the desired separation distance. The larger the number of robots, the better the formation approximates the continuous curve, meaning the approach is *scalable*. For simplicity, let's suppose that the robots are fully actuated and ignore the inertial effects so that the dynamics of R_i is given by $\ddot{q}_i(t) = u_i$. To derive the control input for R_i, we define the potentials $\Phi_\gamma(q_i)$, $\Phi_-(q_i, q_{i-1})$, and $\Phi_+(q_i, q_{i+1})$. $\Phi_\gamma(\cdot)$ is an attractive potential trying to keep R_i on γ and is a function of the distance of $q_i(t)$ to the closest point on γ, denoted $Q(\gamma, q_i(t))$. $\Phi_+(\cdot)$ and $\Phi_-(\cdot)$ are attractive-repulsive potentials which try to maintain a distance L_γ/N between each pair of robots. Now, the control rule is given by

$$\begin{aligned}u_i(t) &= -\lambda_K\dot{q}_i(t) \\ &- \nabla_{q_i}\Phi_\gamma(q_i) - \nabla_{q_i}\Phi_-(q_i, q_{i-1}) - \nabla_{q_i}\Phi_+(q_i, q_{i+1}) \\ u_0(t) &= -\lambda_K\dot{q}_0(t) \\ &- \nabla_{q_0}\Phi_\gamma(q_0) - \nabla_{q_0}\Phi_+(q_0, q_1) \\ u_{N-1}(t) &= -\lambda_K\dot{q}_{N-1}(t) \\ &- \nabla_{q_{N-1}}\Phi_\gamma(q_{N-1}) - \nabla_{q_{N-1}}\Phi_-(q_{N-1}, q_{N-2})\end{aligned} \tag{51}$$

Define $\Phi(p_1, p_2, d) = (\|p_1 - p_2\| - d)^2$, and let

$\Phi_+(q_i, q_{i+1}) = \Phi(q_i, q_{i+1}, L_\gamma/N)$,

$\Phi_-(q_i, q_{i-1}) = \Phi(q_i, q_{i+1}, L_\gamma/N)$, and

$$\Phi_\gamma(q_i) = \Phi(q_i, Q(\gamma, q_i), 0) \tag{52}$$

Note that

$$\nabla_{p_1}\Phi(p_1, p_2, d) = \sqrt{2\Phi(p_1, p_2, d)}\frac{p_1 - p_2}{\|p_1 - p_2\|} \tag{53}$$

A Lyapunov function candidate for the system is

$$\begin{aligned}\mathcal{V}(q,\tau) &= \frac{1}{2}\sum_{i=0}^{N-1}\dot{q}_i^T\dot{q} \\ &+ \sum_{i=1}^{N-2}\Big[\Phi_{\gamma(q_i(\tau))} + \frac{1}{2}\Phi\Big(q_{i+1}(\tau), q_i(\tau), \frac{L_\gamma}{N}\Big) \\ &\qquad + \frac{1}{2}\Phi\Big(q_i(\tau), q_{i-1}(\tau), \frac{L_\gamma}{N}\Big)\Big] \\ &+ \Phi_\gamma(q_0(\tau)) + \frac{1}{2}\Phi\Big(q_0(\tau), q_1(\tau), \frac{L_\gamma}{N}\Big) \\ &+ \Phi_\gamma(q_{N-1}(\tau)) + \frac{1}{2}\Phi\Big(q_{N-1}(\tau), q_{N-2}(\tau), \frac{L_\gamma}{N}\Big)\end{aligned} \tag{54}$$

Lemma 1: *Let $\mathcal{V}(q,\tau)$ be a Lyapunov function for every $\tau \in [\tau_s, \tau_f]$ and $\mathcal{V}(q_{\text{eq}}(\tau), \tau) = 0$. Let Φ_U and $\Phi_{\gamma U}$ denote bounds on Φ_+ (and Φ_-) and Φ_γ. Also, let $\Phi_{\lambda U}$ be the bound on the kinetic energy of the robots (the maximum velocity they can move with). Thus the set $\{q|\mathcal{V}(q,\tau) \le N(\Phi_U + \Phi_{\gamma U} + \Phi_{\lambda U})\}$ is bounded. Let v be a nominal desired speed of traversal. Let $\dot{\tau}$ be given by*

$$\begin{aligned}\dot{\tau} &= \min\{v, \xi(\tau)\}, \\ \xi(\tau) &= h(\mathcal{V}(q(\tau),\tau)) \\ &- \frac{\delta + N(\Phi_U + \Phi_{\gamma U} + \Phi_{\lambda U})}{(\delta + |\partial\mathcal{V}/\partial\tau|)(\delta + \mathcal{V}(q,\tau))}\sum_{i=0}^{N-1}\frac{\partial\mathcal{V}}{\partial q_i}\dot{q}_i(\tau)\end{aligned} \tag{55}$$

and $\dot{\tau} = 0$ at $\tau = \tau_f$, where $h: \Re^+ \to \Re^+$ has compact support in $\mathcal{V} < (1/2)N(\Phi_U + \Phi_{\gamma U} + \Phi_{\lambda U})$ and $h(0) > 0$. Moreover,

$$\begin{aligned}\frac{\partial\mathcal{V}}{\partial q_i} &= 2(q_i - Q(\gamma, q_i)) \\ &+ \mathcal{B}_i^0\Big(\frac{\|q_i - q_{i-1}\| - L_\gamma/N}{\|q_i - q_{i-1}\|}(q_i - q_{i-1})\Big) \\ &+ \mathcal{B}_i^{N-1}\Big(\frac{\|q_i - q_{i+1}\| - L_\gamma/N}{\|q_i - q_{i+1}\|}(q_i - q_{i+1})\Big)\end{aligned} \tag{56}$$

and

$$\begin{aligned}\frac{\partial\mathcal{V}}{\partial\tau} &= \sum_{i=1}^{N-1} \\ &\Big[2(q_i - Q(\gamma, q_i))\Big(\frac{\partial q_i}{\partial\tau} - \partial\gamma(\gamma^{-1}((Q(\gamma, q_i)), \tau))\Big) \\ &+ \mathcal{B}_i^0\Big(\frac{\|q_i - q_{i-1}\| - L_\gamma/N}{\|q_i - q_{i-1}\|}(q_i - q_{i-1})\Big(\frac{\partial q_i}{\partial\tau} - \frac{\partial q_{i-1}}{\partial\tau}\Big)\Big) \\ &+ \mathcal{B}_i^{N-1}\Big(\frac{\|q_i - q_{i+1}\| - L_\gamma/N}{\|q_i - q_{i+1}\|}(q_i - q_{i+1})\Big(\frac{\partial q_i}{\partial\tau} - \frac{\partial q_{i+1}}{\partial\tau}\Big)\Big)\Big]\end{aligned} \tag{57}$$

In the above, $\mathcal{B}_i^k(r) = r$ for $i \ne k$, and $\mathcal{B}_i^k(r) = 0$ for $i = k$. Then the system is stable and asymptotically converges to $(q, t) = (q_{\text{eq}}(\tau_f), \tau_f)$ and

$$\mathcal{V}(q,\tau) \le N(\Phi_U + \Phi_{\gamma U} + \Phi_{\lambda U}) \tag{58}$$

throughout the path.

Proof: Straightforward application of theorem 4.1 in [4]. Define

$$\gamma_\Sigma(s) = \sum_{i=0}^{N-1}\delta_i(s)\frac{q_{i+1}(t)-q_i(t)}{\|q_{i+1}(t)-q_i(t)\|}(s-s_i) \tag{59}$$

where $\delta_i(s)$ is 1 for $s_i \le s < s_{i+1}$ and zero otherwise. We have

$$\varepsilon_N \le \int_0^1 \|\gamma(s)-\gamma_\Sigma(s)\| ds \tag{60}$$

where ε_N is a function of N, approaching zero as $N \to \infty$. If the conditions in lemma 1 are satisfied, the integral will be minimized.

We also have the following which is similar to lemma 6.3 in [4].

Proposition 1: *Suppose that each vehicle can measure the true local gradient $\nabla_{q_i(t)}\mathcal{F}(q_i(t))$. Assume that the control rule, $\dot{\tau}$, and $\mathcal{V}$ are given by equations (51), (54), and (55), respectively. Suppose N is sufficiently large (ε_N is smaller than some specified bound). Let the dynamics of the virtual contour be given by*

$$\dot{\gamma}(s) = \frac{\partial\gamma(s,\tau)}{\partial\tau}\dot{\tau} \text{ where} \tag{61}$$

$$\begin{aligned}\frac{\partial\gamma(s)}{\partial\tau} &= ((\alpha+\beta\kappa_S(\tau))g(\gamma_s(\tau))) \\ &-\langle\frac{1}{\eta(s)}\Big(\eta_-(s)\frac{\partial g}{\partial\mathcal{F}}(q_{i+1})\nabla_{q_{i+1}}\mathcal{F}(q_{i+1}) \\ &+\eta_+(s)\frac{\partial g}{\partial\mathcal{F}}(q_i)\nabla_{q_i}\mathcal{F}(q_i)\Big), N_s(\tau)\rangle \\ &+\Lambda\Big(s-\frac{1}{2}\Big)\frac{\partial L(\tau)}{\partial\tau}T_s(\tau)\end{aligned} \tag{62}$$

$$\begin{aligned}\partial\gamma(0)/\partial\tau &= g(q_0(\tau))\nabla_{q_0(\tau)}\mathcal{F}(q_0(\tau)) \\ &\quad -(\partial L(\tau)/\partial\tau)\nabla^{\perp}_{q_0(\tau)}\mathcal{F}(q_0(\tau))\end{aligned} \tag{63}$$

$$\begin{aligned}\partial\gamma(1)/\partial\tau &= g(q_{N-1}(\tau))\nabla_{q_{N-1}(\tau)}\mathcal{F}(q_{N-1}(\tau)) \\ &\quad -(\partial L(\tau)/\partial\tau)\nabla^{\perp}_{q_{N-1}(\tau)}\mathcal{F}(q_{N-1}(\tau))\end{aligned} \tag{64}$$

Here, $\eta_+(s) = \|\gamma(s)-q_{i+1}\|$, $\eta_-(s) = \|\gamma(s)-q_i\|$, and $\eta(s) = \eta_+(s)+\eta_-(s)$. Then the formation will asymptotically converge to the desired level set defined by $\mathcal{F}(q) = \mathcal{F}_d$ and described by the curve $\gamma_{\mathcal{F}_d}(\tilde{s})$.

Proof: Equation (62) is the steepest descent direction of evolution for the energy functional

$$\int_0^1 \frac{1}{\eta(s)}(\eta_+(s)g(s_-)+\eta_-(s)g(s_+))ds \tag{65}$$

where s_- denotes the nearest s_i for which $s_i < s$ and $s_+ = s_{i+1}$. But this means that

$$\begin{aligned}&\int_0^1 \frac{1}{\eta(s)}(\eta_+(s)g(\gamma_\Sigma(s))+\eta_-(s)g(\gamma_\Sigma(s)))ds \\ &= \int_0^1 \frac{1}{\eta(s)}(\eta_+(s)+\eta_-(s))g(\gamma_\Sigma(s))ds \\ &= \int_0^1 g(\gamma_\Sigma(s))ds\end{aligned} \tag{66}$$

will also be minimized. But the distance between γ and γ_Σ will be less than some desired value which means that $g(s)$ would also be minimized. Convergence to $\gamma_{\mathcal{F}_d}(\tilde{s})$ is guaranteed because $g(\cdot)$ will stop the curve from evolving beyond it. ❑

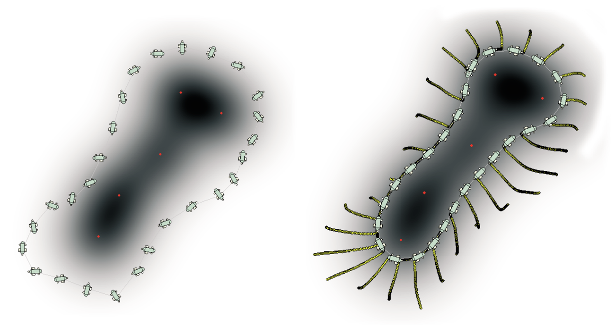

figure 4: Adaptation of closed formations

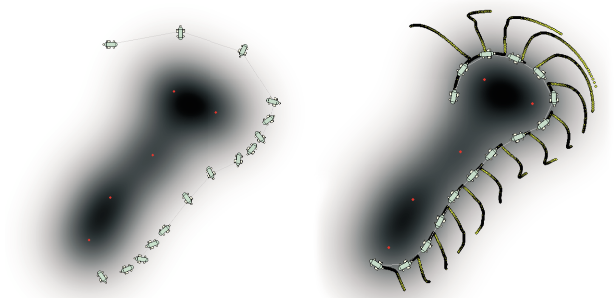

figure 5: Open contour with fixed length

Remark 1: *Equation (29) for $\partial q_i(t)/\partial t$ is equivalent to (51) if we set $u_i = \mathbf{0}$.*

Remark 2: *Lemma 1 also gives conditions on the maximum velocity of a desired moving (non-static) level set. We just need to replace γ with $\gamma_{\mathcal{F}_d}$.*

Remark 3: *It is very important to realize that lemma 1 is meaningful only if the kinetic energy (or the feasible paths) of a vehicle are somehow constrained.*

5. Simulation results

We present some simulation runs exhibiting the fundamental behaviour of the contour formations. The field is composed of five Gaussian overlapping plumes whose centres are shown with red circles. The gradient at each point is thus given by

$$\nabla_q\mathcal{F}(q) = -\Big(\sum_{i=1}^{5}\Big(\frac{(x-x_0)^2}{\sigma^2_{x_i}}\Big)\mathcal{F}_i(q), \sum_{i=1}^{5}\Big(\frac{(y-y_0)^2}{\sigma^2_{y_i}}\Big)\mathcal{F}_i(q)\Big) \tag{67}$$

The sequence of snapshots in figure 4 shows the successful adaptation of a closed formation initially enclosing the desired target level set $\mathcal{F}_d = 12$ (the maximum of $\mathcal{F}(q)$ is approximately 20). The sequence in figure 5 shows a similar scenario but with an open contour, where the length is kept fixed $50(N-1)$. Adaptation will similarly be successful if

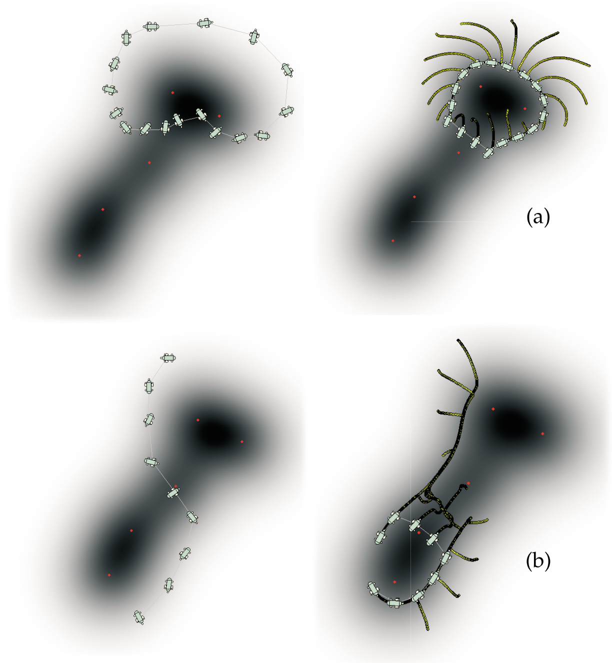

figure 6: Arbitrary initializations with overlap

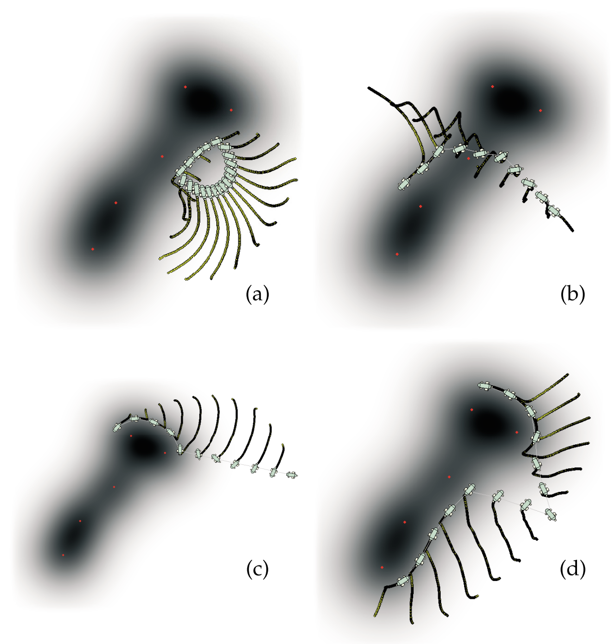

figure 7: Problematic cases

the formations are initialized within the area enclosed by the target level-set.

The next two simulations where the formations start from *not so nice* initial configurations. Figure 6a shows the trace of a closed formation starting from an initial configuration which overlaps with the level set. Figure 6b shows the evolution of an open formation in a similar situation. Note the compaction of the curve before deciding to enclose one of the peaks in the field.

The rest of the simulations serve to demonstrate some of the problematic cases. In figure 7a, the closed formation is initially placed to one side of the level set. In this case, the contour crumbles unto itself. In figure 7b, the gradient is almost co-linear with the tangent to the curve causing the contour to shrink considerably before attempting to adapt. In figure 7c, if the coefficient of tangential velocity is not chosen properly, one end of the curve (closer to the level set) may cross itself. Finally, figure 7d shows a situation where robot R_5 is faulty and cannot move. In this case, parts of the curve may come unacceptably close and eventually cross each other if the β is not big enough or if the initial curvature at the faulty robot site is high. These and other anomalous cases arise due partly to the fact that the robot formation can not imitate the continuous virtual contour quite faithfully, unless N is very large and the formation moves too slowly, (for instance, the computation of the curvature at each point does not go beyond the immediate neighbours) and partly due to the complex interactions with the environment. A major research issue would be to identify all of these problem situations and postulate conditions on initial conditions, number of robots, curve length, field size, field shape,etc. In the simulations, we have put $\alpha = 0$, $\beta = 15000$, $\delta = 1000$, and $\phi = 1500$. Naturally, proper values for these coefficients can play a major role in well-behavedness of the formation. A careful analysis, if possible, can be beneficial. In our simulations, we didn't have to fine-tune them.

6. Conclusion and further research

We showed that decentralized control laws can be derived, based on the general theory of curve evolution in an external field, for autonomous vehicles forming open contours. Some theoretical issues were also discussed. Simulation results were given for the ideal case as well as for anomalous ones. Among the issues which are going to be addressed in forthcoming papers are hybrid automata modelling for synchronous and asynchronous motion, formation initialization, obstacle avoidance and topological designs for gradient estimation by groups of robots, as well as implementation on real hardware. Also of interest is the conditions on the shape and size of a field which will guarantee adaptation without jeopardizing the integrity of the formation. Finally, including noise in measurements and managing faulty vehicles are interesting directions for future research.

References

[1] Kalantar, S., Zimmer, U., *Distributed Shape Control of Homogeneous Swarms of Autonomous Underwater Vehicles*, Submitted to Autonomous Robots, 2005.

[2] Caselles, V., Kimmel, R., Sapiro, G., *Geodesic Active Contours*, International Journal of Computer Vision 22(1), 1997.

[3] Cao, F., Moisan, L., *Geometric Computation of Curvature Driven Plane Curve Evolutions*, SIAM Journal of Numerical Analysis, Vol. 39, No. 2, 2001.

[4] Ogren, P., Fiorelli, E., Leonard, N.E., *Formations with a Mission: Stable Coordination of Vehicle Group Maneuvers*, Proc. Symp. on Mathematical Theory of Networks and Systems, 2002.

[5] Grayson, M.A., *The Heat Equation Shrinks Embedded Plane Curves to Round Points*, Journal of Differential Geometry, 26, 1987.

[6] Cao, F., *Geometric Curve Evolution and Image Processing*, Springer-Verlag, 2003.

[7] Okubo, A., *Diffusion and Ecological Problems: Mathematical Models*, Vol. 10 in Biomathematics Series, Springer-Verlag, 1980.

[8] Randal W. Beard, Jonathan Lawton, Fred Y. Hadaegh: *A Coordination Architecture for Spacecraft Formation Control*, IEEE Transactions on Control Systems Technology, Vol. 9, No. 6, Nov. 2001, pp. 777-790.

[9] R.Olfati-Saber and R.M.Murry: *Distributed Cooperative Control of Multiple Vehicle Formations Using Structural Potential Functions*, The 15th IFAC World Conf., June 2002.

[10] M. Egerstedt, X. Hu: *Formation Constrained Multi-Agent Control*, IEEE Trans. on Robotics and Automation, Vol. 17, No. 6, Dec. 2001, pp. 947-951.

[11] Marthaler, D., Bertozzi, A. L., *Tracking environmental level sets with autonomous vehicles*, Recent Developments in Cooperative Control and Optimization, Kluwer, 2004.

[12] Robinett, R.D., Hurtado, J.E., *Stability and control of Collective Systems*, Journal of Intelligent and Robotic Systems, 39, 2004.

[13] Belta C., Kumar V.: *Towards abstraction and control for large groups of robots*. 2nd International Workshop on Control Problems in Robotics and Automation, Las Vegas, NV, Dec. 2002.

[14] Gazi, V., Passino, K.M., *Stability Analysis of Social Foraging Swarms: Combined Effects of Attractant/Repellent Profiles*, Proc. of the 41st IEEE Conf. on Decision and Control, 2002.

[15] Pereira, G.A.S., Das, A.K., Kumar, V., Campos, M. F. M., *Formation control with configuration space constraints* in Proc. of the IEEE/RJS Int. Conf. on Intelligent Robots and Systems (IROS'03), 2003.

[16] http://users.rsise.anu.edu.au/~serafina/